AMERICAN SOCIETY FOR MICROBIOLOGY | Infection and Immunity®

HOST RESPONSE AND INFLAMMATION

Position-Specific Secondary Acylation Determines Detection of Lipid A by Murine TLR4 and Caspase-11

Erin M. Harberts,[a] Daniel Grubaugh,[b] Daniel C. Akuma,[b] Sunny Shin,[c] Robert K. Ernst,[a] Igor E. Brodsky[b]

[a]Department of Microbial Pathogenesis, University of Maryland, School of Dentistry, Baltimore, Maryland, USA
[b]Department of Pathobiology, University of Pennsylvania School of Veterinary Medicine, Philadelphia, Pennsylvania, USA
[c]Department of Microbiology, University of Pennsylvania Perelman School of Medicine, Philadelphia, Pennsylvania, USA

Erin M. Harberts and Daniel Grubaugh contributed equally. Author order was determined by reverse alphabetical order.

ABSTRACT Immune sensing of the Gram-negative bacterial membrane glycolipid lipopolysaccharide (LPS) is both a critical component of host defense against bacterial infection and a contributor to the hyperinflammatory response, potentially leading to sepsis and death. Innate immune activation by LPS is due to the lipid A moiety, an acylated di-glucosamine molecule that can activate inflammatory responses via the extracellular sensor Toll-like receptor 4 (TLR4)/myeloid differentiation 2 (MD2) or the cytosolic sensor caspase-11 (Casp11). The number and length of acyl chains present on bacterial lipid A structures vary across bacterial species and strains, which affects the magnitude of TLR4 and Casp11 activation. TLR4 and Casp11 are thought to respond similarly to various lipid A structures, as tetra-acylated lipid A structures do not activate either sensor, whereas hexa-acylated structures activate both sensors. However, the precise features of lipid A that determine the differential activation of each receptor remain poorly defined, as direct analysis of extracellular and cytosolic responses to the same sources and preparations of LPS/lipid A structures have been limited. To address this question, we used rationally engineered lipid A isolated from a series of bacterial acyl-transferase mutants that produce novel, structurally defined molecules. Intriguingly, we found that the location of specific secondary acyl chains on lipid A resulted in differential recognition by TLR4 or Casp11, providing new insight into the structural features of lipid A required to activate either TLR4 or Casp11. Our findings indicate that TLR4 and Casp11 sense nonoverlapping areas of lipid A chemical space, thereby constraining the ability of Gram-negative pathogens to evade innate immunity.

KEYWORDS LPS, TLR4, caspase-11, inflammasome, lipid A, pyroptosis, sepsis

Innate immune receptors alert the host to infection through sensing of pathogen-associated molecular patterns (PAMPs). Lipopolysaccharide (LPS) and lipooligosaccharide (LOS) are essential structural components of Gram-negative bacterial membranes that activate the extracellular membrane-bound Toll-like receptor 4 (TLR4)/myeloid differentiation 2 (MD-2) signaling complex (here called TLR4) and the intracellular receptors human caspase-4/5 and mouse caspase-11 (Casp11) (1). Mice lacking either TLR4 or Casp11 are highly susceptible to Gram-negative bacterial infection and, conversely, are resistant to LPS-driven models of acute sepsis (2–5). LPS is composed of O-antigen, a highly variable glycosyl structure attached to a more conserved core oligosaccharide, which together are anchored into the outer leaflet of the outer membrane by the highly conserved lipid A moiety, whereas LOS contains the core oligosaccharide portion and lacks O-antigen. Lipid A, the membrane anchor of LPS/LOS, is sensed by both TLR4 and caspase-11/4/5 and is thus a primary driver of endotoxic shock during Gram-negative bacterial infection

Editor Andreas J. Bäumler, University of California, Davis

Address correspondence to Igor E. Brodsky, ibrodsky@vet.upenn.edu, or Robert K. Ernst, Rkernst@umaryland.edu.

The authors declare no conflict of interest.

For a companion article on this topic, see https://doi.org/10.1128/IAI.00208-22.

Received 26 May 2022
Accepted 2 June 2022
Published 14 July 2022

(6, 7). Lipid A is composed of a $\beta(1\rightarrow6)$-linked di-glucosamine backbone, two 3-OH acyl groups attached at each of the N-linked (2 and 2′) and O-linked (3 and 3′ position) positions, and two terminal phosphate moieties at the 1 and 4′ positions on the di-glucosamine backbone. The acyl chains bound directly to glucosamine are termed primary acyl chains, which can in turn be modified with addition of secondary acyl chains via ester linkages (8). The number, position, and length of the acyl chains vary widely across different species and strains of bacteria, as well as in response to environmental conditions (9). Importantly, these structural differences have a direct effect on the magnitude and duration of the innate immune response, but the precise effect of specific acyl chain additions/removals has not yet been described (10).

Extracellular LPS is detected by the plasma membrane-localized TLR4/MD2 receptor signaling complex. When not bound by a ligand, TLR4 exists as a monomer spanning the plasma membrane with extra- and intracellular domains. Receptor complex initiation begins when LPS is bound by lipopolysaccharide-binding protein (LBP), which then transfers LPS to CD14 and subsequently the MD-2 coreceptor. MD-2 presents LPS to TLR4, causing a conformational change that enables dimerization of TLR4 monomers. This brings the TLR4 cytoplasmic signaling domains into proximity with each other and propagates downstream signaling (11, 12). The structure of lipid A determines binding to the TLR4/MD-2 complex (13, 14). In general, hexa-acylated lipid A structures are known agonists of TLR4, whereas tetra-acylated lipid A is antagonistic (15). In addition to acyl chain numbers, lipid A acyl chain length has an impact on downstream signal strength. This has been shown previously in mutants of *Haemophilus influenzae*, *Neisseria meningitidis*, *Neisseria gonorrhoeae*, and *Salmonella enterica* serotype Typhimurium lacking the secondary lipid A acyltransferase HtrB/LpxL, resulting in a penta-acylated lipid A lacking $C_{14:0}$ (myristate), leading to reduced inflammatory potential and virulence (16–22). In addition, the acylation state of lipid A, as well as alterations in modifications to the terminal phosphate moieties, can alter innate immune recognition. For example, the lipid A phosphatases, LpxE and LpxF from *Francisella* species, are site-specific enzymes that remove either the 1- or 4′-position phosphate groups, respectively, and affect recognition by TLR4 and resistance to cationic antimicrobial molecules (23–29). Notably, while both human and mouse TLR4 detect extracellular LPS, they exhibit species-specific differences in their responsiveness to distinct lipid A structures, as the human MD2/TLR4 complex is less responsive than mouse TLR4 to underacylated forms of lipid A (30, 31). Furthermore, differential TLR4 activation between temperature-regulated lipid A structures, synthesized by *Yersinia pestis* is more pronounced in human cells, which do not recognize tetra-acylated lipid A, compared to mouse cells, which maintain limited recognition of tetra-acylated lipid A (32), highlighting the selectivity of the structure-activity relationship of lipid A with the TRL4/MD-2 complex.

While TLR4 senses the presence of extracellular LPS, the intracellular protein Casp11 in mice, and its human orthologs CASP4 and CASP5, detect LPS that enters the cytosol due to vacuolar escape by cytosolic pathogens, such as *Burkholderia pseudomallei* (33), or disruption of the vacuolar membrane by bacterial or cellular factors (4, 7, 34, 35). Unlike TLR4, caspases do not strictly require a coreceptor for detecting LPS, although recent studies have revealed an important accessory role for guanylate binding proteins (GBPs) in full activation of this pathway (36–39). Briefly, lipid A binds directly to the caspase activation and recruitment domain (CARD) of Casp11, leading to its oligomerization (7), followed by proximity-induced autoprocessing and formation of the noncanonical inflammasome (40). Activated Casp11 subsequently cleaves downstream effector molecules, including gasdermin D (GSDMD), leading to formation of GSDMD pores in the plasma membrane that mediate pyroptotic cell death and release of interleukin-1 (IL-1) family cytokines and intracellular alarmins (41, 42). While the structural requirements of lipid A bound to MD-2 and TLR4 are better understood (43), the structural requirements and the contribution of individual lipid A components to Casp11 activation are undefined. Furthermore, because lipid A structure varies greatly among bacterial species and very little direct comparison of TLR4 and Casp11 responsiveness

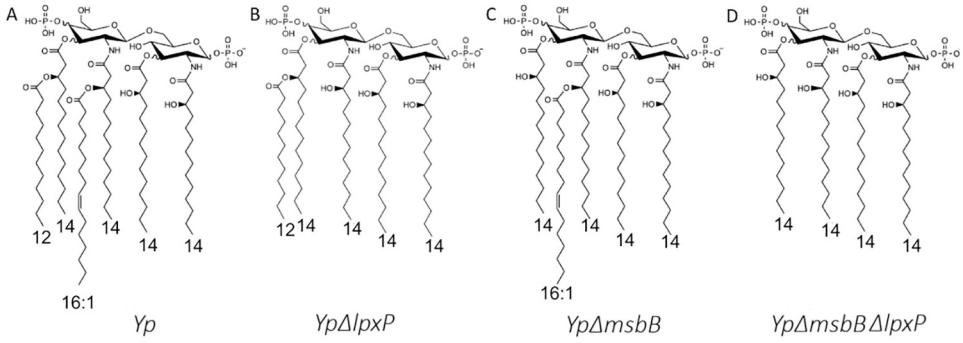

FIG 1 Chemical structures of lipid A molecules. (A to D) Structures are shown for WT *Yersinia pestis* (A), *Y. pestis* Δ*lpxP* (B), *Y. pestis* Δ*msbB* (C), and *Y. pestis* Δ*lpxP* Δ*msbB* (D) lipid A, all grown at 26°C. When describing these molecules, the 1-position is where the phosphate group on the right side of the molecule is added, with the carbons in the ring being sequentially numbered moving down and to the left. Similarly, the 1′-position is where the link is made between the two carbon rings again numbered sequentially, with the 2′-position being the next carbon down and to the left. The second phosphate group is added at the 4′-position.

to individual lipid A structures exist, we have only a limited understanding of how distinct lipid A structures activate these two endotoxin sensing pathways.

Here, we used defined biosynthetic mutants of *Y. pestis* that lack one or both of the secondary acyltransferases, MsbB/LpxM and LpxP, to generate defined structures of bacterial lipid A, allowing us to directly dissect the contribution of specific lipid A secondary acyl-chain modifications to activation of murine TLR4 and Casp11. *Y. pestis* synthesizes LOS due to a mutation in O-antigen synthesis (44). Intriguingly, we found that in murine cells, position-specific addition of a fifth acyl chain to lipid IVa by either MsbB or LpxP acyltransferases converts nonactivating tetra-acylated lipid IVa to a specific agonist of either Casp11 or TLR4, respectively. Collectively, these findings indicate that mouse Casp11 and TLR4 are differentially activated by structurally distinct forms of lipid A. In particular, the location of secondary acyl chains differentially impacts the ability of these two pathogen sensors to detect lipid A species. These findings highlight the overlapping constraints that these innate immune LPS sensing molecules place on the lipid A structures of pathogens, thereby limiting the ability of pathogens to evade innate immune detection.

RESULTS

Distinct penta-acylated lipid A species enable defined analysis of extracellular and cytosolic innate immune responses to endotoxin. Lipid A structure varies broadly among bacterial species (9), many of which undergo regulated changes to their lipid A in response to environmental conditions, including temperature and pH (45). In particular, *Yersinia pestis* grown at an environmental temperature (26°C) produces a hexa-acylated lipid A, whereas lipid A prepared from *Y. pestis* grown at mammalian body temperature (37°C) is tetra-acylated due to the absence of secondary acyl chains (32, 46). *Y. pestis* lipid A structure determines how the bacteria are recognized by the host and correlates with pathogenicity (47). When grown at mammalian temperature, *Y. pestis* evades immune recognition by TLR4, an adaptation that allows for evasion of innate immune defense and enhances virulence in mammals (48, 49). In *Y. pestis*, the addition of the secondary C_{12} and $C_{16:1}$ acyl chains is mediated by the acyltransferases MsbB and LpxP, respectively (Fig. 1) (50). Thus, loss of LpxP results in the absence of the O-linked 16:1 acyl-chain on the 2′ 3-OH 14-carbon acyl-chain, whereas deletion of *msbB* results in the loss of the O-linked 12-carbon acyl-chain on the 3′ 3-OH 14-carbon acyl-chain. Deletion of both *msbB* and *lpxP* results in a 3-OH 14-carbon tetra-acylated lipid A. While hexa-acylated lipid A structures are detected by both TLR4 and Casp11, and tetra-acylated lipid A structures are not detected by either, penta-acylated LPS structures are variable with respect to their ability to activate TLR4 and Casp11 (4, 8, 51, 52). The underlying basis for selective responses of intra- and extracellular LPS

sensing pathways to different LPS structures is therefore not clear. Moreover, responses of murine and human extra- and intracellular LPS sensing pathways have been studied in response to similar lipid A structures isolated from different bacterial species under different growth conditions, thus limiting the ability to make direct comparisons between murine and human systems. We previously established a system in *Y. pestis* to purify defined LOS structures that have distinct abilities to stimulate TLR4-dependent responses (53). Here, we took advantage of this approach to produce LOS structures that are identical other than the positioning and number of secondary acyl chains (Fig. 1), thereby enabling us to define the innate immune responses to closely related penta-acylated lipid A structures in murine and human systems (54).

***lpxP*-mediated lipid A modifications allow for TLR4 activation.** To dissect the contribution of specific acyl chain lipid A modifications to TLR4 signaling, the HEK-Blue mTLR4 reporter cell line was used to define TLR4-dependent signaling in response to LOS and lipid A isolated from wild-type (WT) *Y. pestis* and acyltransferase mutant strains lacking one or both of *lpxP* and *msbB*. Notably, LOS isolated from the *Y. pestis* Δ*msbB* mutant, which lacks the secondary C_{12} acyl chain at the 3′ position, activated TLR4 signaling in HEK-Blue mTLR4 cells similarly to the proinflammatory WT *Y. pestis* hexa-acylated structure, whereas penta-acylated lipid A derived from *Y. pestis* Δ*lpxP*, lacking the secondary $C_{16:1}$ acyl chain at the 2′ position, was a poor TLR4 activator, similar to tetra-acylated lipid A isolated from the *Y. pestis* Δ*msbB* Δ*lpxP* double mutant (Fig. 2A). This was the case for both lipid A and corresponding LOS molecules, though WT *Y. pestis* LOS showed higher activity, indicating that the oligosaccharide moieties beyond lipid A do not fundamentally affect TLR4 recognition. Murine RAW-Blue cells, which express an NF-κB-driven secreted alkaline phosphatase, also exhibited elevated activation in response to LOS and lipid A from *Y. pestis* Δ*msbB* compared to WT *Y. pestis*- or *Y. pestis* Δ*lpxP*-derived lipid A and LOS (Fig. 2B), though the differences in activation by different TLR4 ligands were not as pronounced in the RAW-Blue cell line. This may be due to differences in the level of endogenous TLR4 expression in RAW macrophage-like cells in comparison to HEK293 cells where the receptor is highly expressed.

While the reporter cells give a clear picture of the specific contributions of TLR4, these cell lines may not accurately reflect cytokine secretion by primary immune cells. Thus, we stimulated murine bone marrow-derived macrophages (BMDMs) with each lipid A molecule and measured cytokine secretion using cytometric bead arrays. Consistent with the reporter studies, BMDMs stimulated with lipid A from WT *Y. pestis* and *Y. pestis* Δ*msbB* produced significantly higher levels of cytokines IL-6 (Fig. 2C), tumor necrosis factor alpha (TNF-α) (Fig. 2D), and IL-10 (Fig. 2E) than either *Y. pestis* Δ*lpxP* or the tetra-acylated *Y. pestis* Δ*msbB* Δ*lpxP*. These findings are consistent with previous observations that penta-acylated LPS structures containing acyl chains of 16 carbons or longer are generally weak agonists for TLR4/MD-2, which is attributed to their poor fit within the MD-2 binding pocket (14). Together, these findings identify a previously unknown minimum stimulatory component of lipid A signaling through TLR4 and demonstrate that penta-acylated lipid A containing a secondary acyl-chain at the 2′ position, but not the 3′, position is sufficient to activate TLR4 signaling.

***msbB*-dependent acylation of lipid A is required for activation of Casp11-dependent cell death.** Casp11 is the intracellular sensor of lipid A in mice. While both TLR4 and Casp11 sense lipid A, the structural requirements for Casp11-mediated detection of lipid A are poorly defined. To define the role of specific lipid A modifications in Casp11 activation, we primed wild-type (C57BL/6) and Casp11-deficient (*Casp11*$^{-/-}$) mouse (BMDMs) with Pam3CSK4 for 4 h followed by transfection with LOS containing the defined lipid A structures in Fig. 1 and assessed the ability of distinct lipid A structures to activate Casp11 by assaying Casp11-dependent cell death using a lactate dehydrogenase release assay (LDH). As expected, hexa-acylated lipid A induced cell death in WT BMDMs relative to *Casp11*$^{-/-}$ BMDMs at each of the concentrations tested (Fig. 3A), whereas *Y. pestis* Δ*msbB* Δ*lpxP*-derived tetra-acylated lipid A did not (Fig. 3B). However, in contrast to its activation of TLR4, *Y. pestis* Δ*msbB*-derived penta-acylated lipid A, which lacks a C_{12} secondary acyl chain on the 3′ O-linked primary acyl group (Fig. 1), induced

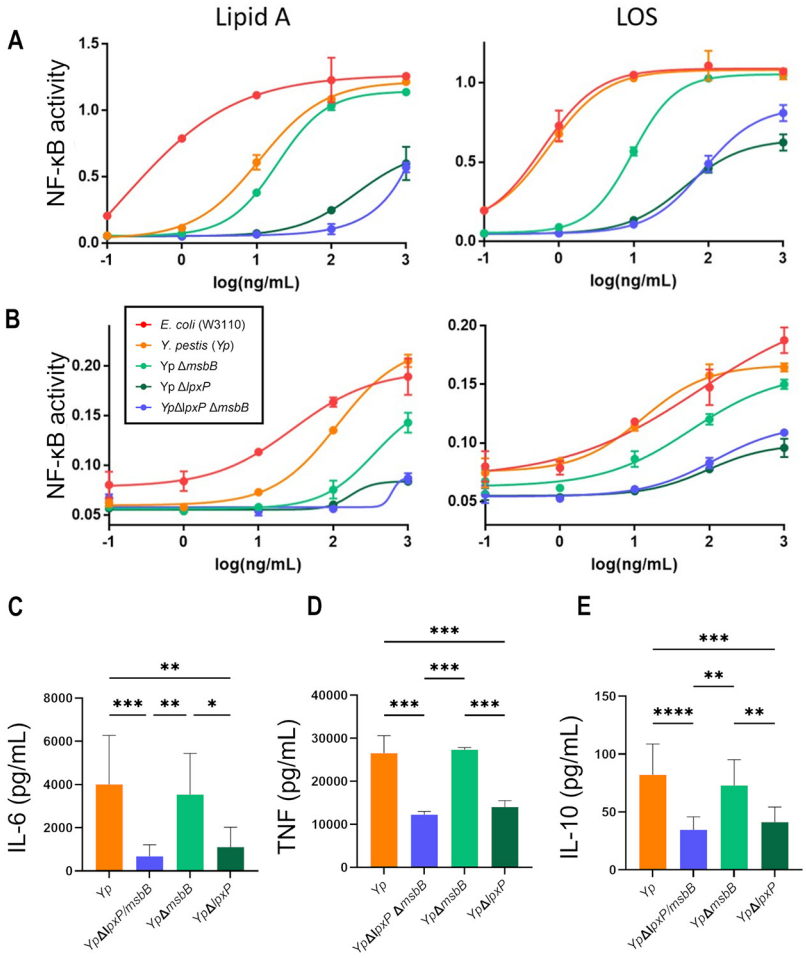

FIG 2 LPS and lipid A from *Yersinia pestis* Δ*msbB* but not Δ*lpxP* agonize TLR4. (A and B) LPS/LOS and lipid A extracted from *Escherichia coli* (red), WT *Y. pestis* (orange), *Y. pestis* Δ*msbB* (light green), *Y. pestis* Δ*lpxP* (dark green), and *Y. pestis* Δ*msbB* Δ*lpxP* (blue) were cultured with HEK-Blue mTLR4 cells (A) or RAW-Blue cells (B) for 18 h. Secreted alkaline phosphatase (SEAP) activity is graphed over the 5-log concentration range tested. The averages ± standard deviation (SD) of biological duplicates are shown; data are representative of three independent experiments. (C to E) Lipid A from each variant was added to BMDMs at a concentration of 100 ng/mL and incubated for 24 h. Levels of the indicated cytokines in cell supernatant were measured by cytometric bead array. Data are presented as means (± SD) of experiments performed in triplicate. Data are representative of 2 to 3 independent experiments. *, $P < 0.05$; **, $P < 0.01$; ***, $P < 0.001$; ****, $P < 0.0001$; one-way analysis of variance (ANOVA) followed by Tukey's multiple-comparison test.

minimal levels of cell death (Fig. 3C). This finding is consistent with prior observations that penta-acylated lipid A structures, particularly those containing C_{16}-length acyl chains, are generally weak activators of Casp11 or are Casp11 antagonists (4) and contrasts with the ability of lipid A derived from *Y. pestis* Δ*msbB* to activate TLR4.

Intriguingly, penta-acylated lipid A derived from *Y. pestis* Δ*lpxP* and therefore lacking the secondary acyl group linked to the 2′ amino group acyl chain (Fig. 1) induced significantly increased levels of cell death in WT BMDMs, compared to *Casp11*$^{-/-}$ BMDMs and nearly the same extent of cell death as hexa-acylated LPS (Fig. 3D). Additionally, *Y. pestis* Δ*lpxP* LOS induced significantly higher levels of cell death than *Y. pestis* Δ*msbB* across a wide dose range (Fig. 3E), indicating that a single acyl chain position alters the capacity of penta-acylated LOS to activate Casp11. Notably, the same pattern of differential stimulatory capacity was observed when coadministered with *Listeria monocytogenes* (34) (see Fig. S1 in the supplemental material), indicating that differences in transfection efficiency are unlikely to account for the difference observed

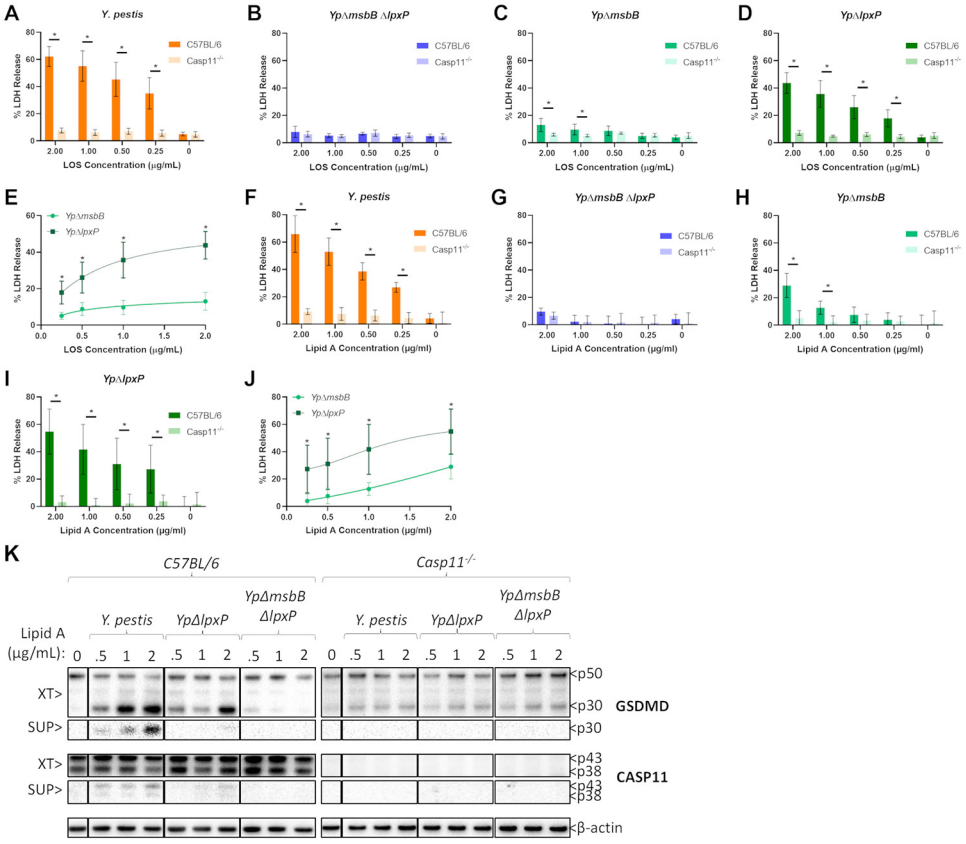

FIG 3 The secondary acyl chain position determines the ability of penta-acylated LPS to induce Casp11-dependent cell death. (A to D and F to I) Pam3CSK4-primed BMDMs from wild-type (C57BL/6) and Casp11-deficient (*Casp11*$^{-/-}$) mice were transfected with the indicated concentrations of purified LOS (A to D) or lipid A (F to I) isolated from the indicated *Y. pestis* mutants. Then, 20 h after transfection, cell supernatants were assayed for lactate dehydrogenase activity. Lactate dehydrogenase activity was determined relative to cells lysed using Triton X-100. Data are presented as the mean (± SD) of three independent experiments performed in triplicate. For panels A to D and F to I: *, significant difference between C57BL/6 and *Casp11*$^{-/-}$, $P < 0.05$, *t* test using the Holm-Sidak method for multiple hypothesis testing. (E and J) The significant difference between the two penta-acylated structures *Y. pestis* Δ*msbB* and *Y. pestis* Δ*lpxP*, $P < 0.05$, *t* test using Holm-Sidak method for multiple hypothesis testing. (K) Pam3CSK4-primed BMDMs from wild-type (C57BL/6) and Casp11-deficient (*Casp11*$^{-/-}$) mice were transfected with the indicated concentrations of purified lipid A from the indicated mutants as described above, and whole-cell lysates (XT) and supernatants (sup) were isolated 20 h posttransfection and analyzed by Western blotting for gasdermin D (GSDMD) and Casp11 processing as indicated. *β*-actin is indicated as a loading control.

in their stimulatory capacity. Altogether, these findings suggest that the presence or absence of secondary acyl chain modifications is a major determinant of Casp11 activation.

LOS contains an oligosaccharide moiety which could impact Casp11-dependent innate responses (55). To test whether the difference in Casp11 activation levels between the various LOS molecules was directly attributable to the lipid A acylation state, we assayed Casp11-dependent cell death in response to cytosolic delivery of purified lipid A lacking core oligosaccharide from each strain. Consistent with our findings using LOS, both *Y. pestis* and *Y. pestis* Δ*lpxP* lipid A structures induced robust cell death, whereas lipid A from *Y. pestis* Δ*msbB* largely failed to induce cell death except at the highest concentrations, and tetra-acylated lipid A derived from *Y. pestis* Δ*msbB* Δ*lpxP* failed to induce cell death entirely (Fig. 3F to I). As with their LOS structural counterparts, *Y. pestis* Δ*lpxP*-derived lipid A again induced significantly more cell death than lipid A derived from *Y. pestis* Δ*msbB* (Fig. 3J). Notably, both *Y. pestis*- and Δ*lpxP*-derived lipid A induced significant GSDMD cleavage in cell lysates, whereas Δ*msbB* Δ*lpxP*-derived lipid A did not, and only *Y. pestis* induced robust release of cleaved GSDMD into the supernatant (Fig. 3K), in keeping with their relative levels of cell death induction. Altogether, these data demonstrated that the number and

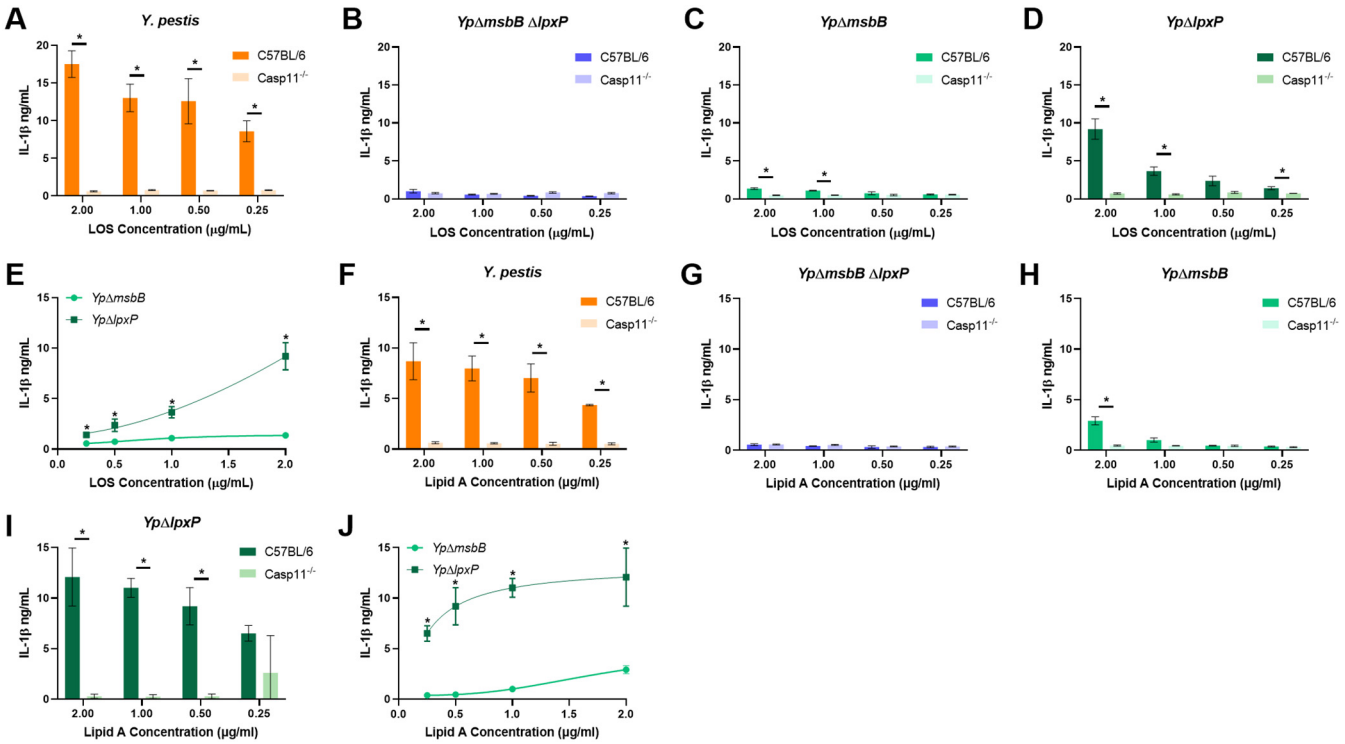

FIG 4 Secondary acyl chain positions contribute to the ability of penta-acylated LPS to induce IL-1β secretion. (A to D) Pam3CSK4-primed BMDMs from wild-type (C57BL/6) and Casp11-deficient (*Casp11*$^{-/-}$) mice were transfected with the indicated concentrations of LOS (A and C) or lipid A (B and D). Then, 20 h after transfection, cell supernatants were collected and the IL-1β concentration was measured using ELISA. Data are representative of three independent experiments performed in triplicate. For panels A and B: *, significant difference between C57BL/6 and *Casp11*$^{-/-}$, $P < 0.05$, *t* test using Holm-Sidak method for multiple hypothesis testing. For panels C and D: *, significant difference between *Y. pestis* Δ*msbB* and *Y. pestis* Δ*lpxP*, $P < 0.05$, *t* test using Holm-Sidak method correction for multiple hypothesis testing.

position of acyl chains is the primary determinant for Casp11 activation by cytosolic bacterial LOS or lipid A.

***MsbB*-dependent acylation of lipid A is required for activation of Casp11-dependent IL-1β secretion.** Activation of the Casp11 noncanonical inflammasome triggers the processing and release of IL-1 family cytokines via secondary activation of NLRP3 (35). To directly test the contribution of acyl chain position to IL-1β release, we assessed IL-1β levels in the supernatants of BMDMs transfected with LOS variants. As expected, LOS from WT *Y. pestis* induced significant IL-1β release at all four tested concentrations (Fig. 4A), while tetra-acylated LOS purified from *Y. pestis* Δ*msbB* Δ*lpxP* bacteria failed to induce IL-1β release relative to *Casp11*$^{-/-}$ control BMDMs (Fig. 4B). LOS derived from the *Y. pestis* Δ*msbB* (Fig. 4C) mutant led to minimal IL-1β release, compared to *Y. pestis* Δ*lpxP* (Fig. 4D), which induced significant Casp11-dependent IL-1β secretion (Fig. 4E). Similar results were observed following transfection of purified lipid A, with WT *Y. pestis* and *Y. pestis* Δ*lpxP* lipid A leading to IL-1β release at all concentrations and *Y. pestis* Δ*msbB* lipid A only inducing IL-1β secretion at the highest concentrations (Fig. 4F to J). Taken together, these data indicate that the Casp11 inflammasome response to penta-acylated LOS/lipid A requires a secondary O-linked acylation at the 3′ acyl chain, and that, similar to TLR4, the position of secondary acylation plays a critical role in determining the ability to activate Casp11.

LOS from Δ*msbB Yersinia* weakly antagonizes Casp11. LPS from *Helicobacter pylori* and *Rhizobium galegae*, which also produce primarily a penta-acylated lipid A structure similar to that produced by *Y. pestis* Δ*msbB*, are known to inhibit activation of Casp11 by agonist LPS when cotransfected into BMDMs (4, 56). In contrast, lipid IVa, a structure similar to *Y. pestis* Δ*msbB* Δ*lpxP* lipid A, does not block Casp11 activation by agonist LPS (4). To test whether *Y. pestis* Δ*msbB* lipid A could also block Casp11 signaling, we transfected BMDMs with increasing concentrations of *Y. pestis* Δ*msbB* or *Y. pestis*

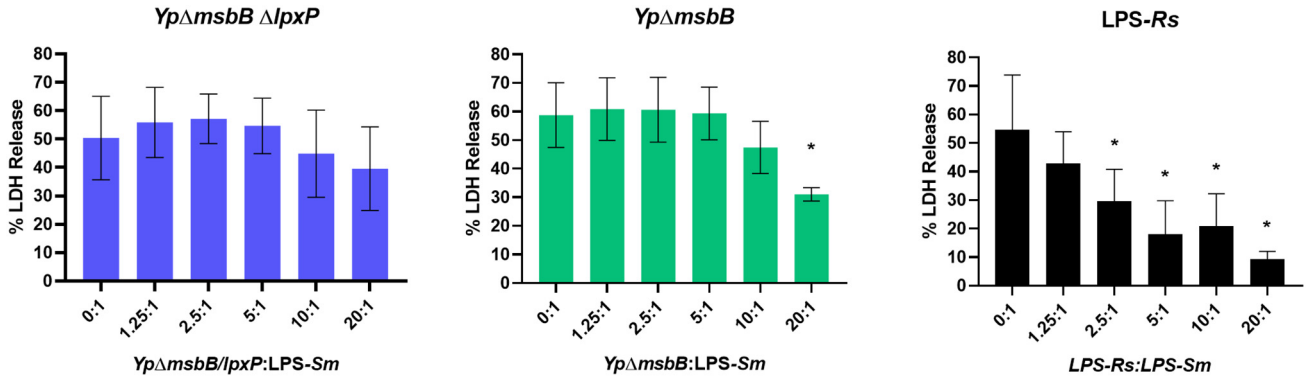

FIG 5 Penta-acyl LPS molecules differ in their ability to inhibit Casp11. BMDMs were primed with Pam3CSK4 and then transfected with 1 μg/mL LPS from *Salmonella* Minnesota (LPS-*Sm*) alone or with increasing doses of one of the indicated hypo-acylated LPS molecules. (LPS-*Rs* indicates LPS from *Rhodobacter sphaeroides*.) Then, 20 h after transfection, cell supernatants were assayed for lactate dehydrogenase activity. Lactate dehydrogenase activity was determined relative to cells lysed using Triton X-100. Data are presented as averages ($\pm$ SD) of three independent experiments performed in triplicate. *, significant difference from LPS-*Sm* alone, $P < 0.05$, one-way ANOVA with Dunnet's multiple-comparison test.

Δ*msbB* Δ*lpxP* LOS or *Rhodobacter sphaeroides* (LPS-*Rs*) LPS in the presence of the potent Casp11 agonist *Salmonella enterica* serotype Minnesota LPS (34). As expected, tetra-acylated *Y. pestis* Δ*msbB* Δ*lpxP* LOS failed to inhibit cell death in response to Casp11 agonist LPS, whereas LPS-*Rs*, which binds but does not activate Casp11, exhibited a strong dose-responsive ability to block cell death. Despite being penta-acylated, we found that *Y. pestis* Δ*msbB* LOS acted more like the *Y. pestis* Δ*msbB* Δ*lpxP* LOS, partially blocking Casp11 activation at only at the highest concentrations (Fig. 5). These data indicate that acyl chain number alone does not determine Casp11 antagonism, which involves as-yet-to-be-defined structural properties of lipid A.

DISCUSSION

Lipid A, a major component of the outer membrane of Gram-negative bacteria, is recognized by the host innate immune system, contributing both to pathogen control and inflammatory pathology during disease. The innate immune system senses lipid A through two distinct but functionally linked receptors, TLR4 and Casp11. While lipid A structures that are agonists or nonagonists for Casp11 and TLR4 are considered to be similar, the precise rules that determine which lipid A structures activate Casp11 and how these structures are recognized are not fully understood. Importantly, the lack of a standardized series of lipid A molecules that are uniformly isolated and prepared has limited our understanding of these processes. Here, we employed a series of defined lipid A structures derived from specific mutants of *Y. pestis* to investigate the precise link between acylation state and intracellular and extracellular LPS sensing. Our results indicate that the $C_{16:1}$ O-linked acyl chain of *Y. pestis* lipid A is necessary for activation of TLR4, while the shorter 12-carbon chain at the 3′ position is mostly dispensable (Fig. 2). Conversely, we found that the majority of Casp11 activation induced by hexa-acylated *Y. pestis* is due to the presence of the secondary acyl chain at the 3′ position of the di-glucosamine backbone (Fig. 3 and 4). Thus, each of these penta-acylated structures represents a minimum stimulatory lipid A structure for TLR4 and Casp11. In addition, we found that the minimally TLR4-activating penta-acyl structure also had some weak antagonistic activity against Casp11 (Fig. 5). In the case of TLR4, differences in stimulation between the two penta-acyl structures may reflect differential binding of these molecules within the hydrophobic pocket of the MD-2 coreceptor (43). The long 16:1-carbon chain, in particular, may stabilize binding, leading to enhanced TLR4 signaling. Alternatively, the differences between the penta-acyl structures may be attributable to interactions with molecules upstream of MD2, as LPS structure has been shown to affect the ability of CD14 to bind and transfer endotoxin. However, the

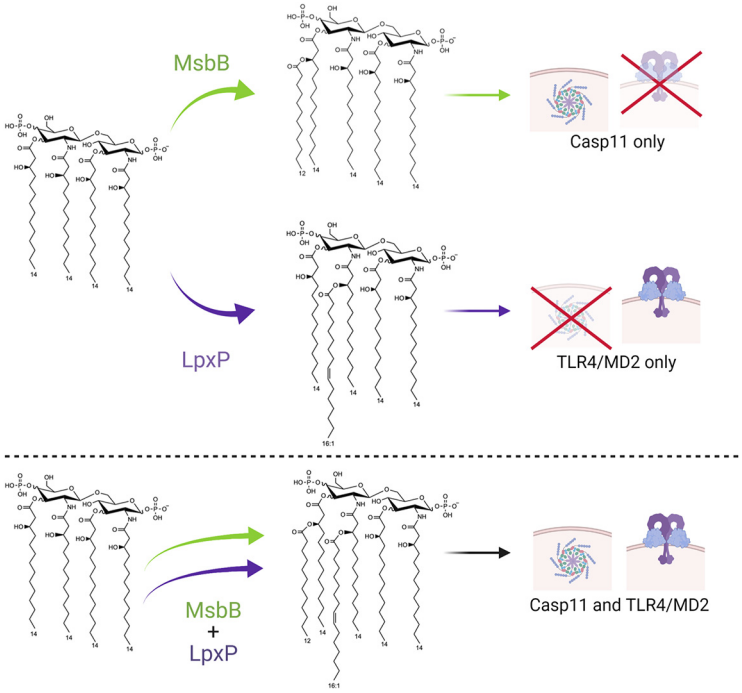

FIG 6 Acylation patterns of lipid A from *Yersinia pestis* determine differential TLR4/MD2 and caspsase-11 activation (created with BioRender.com).

structural reasons for the importance of the 3′ secondary acyl chain in Casp11 activation are currently less clear.

Previous work on Casp11 recognition of LPS has shown that the number of acyl chains in the lipid A moiety of LPS is important for determining whether that particular structure can activate the noncanonical inflammasome. Based on these studies, it is currently thought that hepta- or hexa-acylated lipid A activates Casp11, whereas structures with fewer acyl chains do not. Unexpectedly, we identified penta-acylated lipid A structures that, despite having the same number of acyl chains, differ greatly in their ability to activate Casp11 and exhibit an inverse relationship in their ability to activate TLR4 (Fig. 6). Our results indicate that Casp11 recognition depends on the position and length of secondary acyl chains in the lipid A molecule. *Chlamydia*, *Rhodobacter*, and *Rhizobium* species produce lipid A molecules that do not activate Casp11, and in the case of *Rhodobacter* and *Rhizobium* have been shown to inhibit Casp11 activation. Intriguingly, the structures of these lipid A molecules are similar to those of *Y. pestis* Δ*msbB* in that they are penta-acylated with their sole secondary acyl chain at the 2′ position. These results suggest that the presence of a secondary acyl chain at the 3′ position may be a general requirement for activation Casp11 activation, whereas a secondary acyl chain at the 2′ position may be a feature of inhibitory lipid A molecules (4, 23, 54, 57, 58).

A recent study that analyzed the ability of commercial preparations of *Bordetella pertussis* LPS to activate TLR4 and Casp11 found that although *B. pertussis* LPS, which is primarily, but not exclusively, composed of penta-acylated LPS that lacks a secondary 3′ acyl chain, stimulated lower levels of IL-1α, it was still able to induce robust LDH release (52). Our finding that mixtures of nonstimulatory and stimulatory LPS still trigger robust noncanonical inflammasome activation indicate that analysis of noncanonical inflammasome responses to lipid A require the use of lipid A preparations that contain uniform structures.

Our study reveals for the first time that distinct secondary acyl chains mediate the activation of murine TLR4 and the Casp11/GSDMD activation pathway by lipid A (Fig. 2 and 4). Unlike the enteric *Yersinia* species, *Y. pestis* lacks *lpxL*, which encodes

a late acyltransferase that adds secondary acyl chains in other Gram-negative *Enterobacteriaceae* (48). The absence of this acyltransferase, combined with the coordinate downregulation of both the *msbB* and *lpxP* genes, allows *Y. pestis* to modify its lipid A and escape innate immune surveillance to establish a productive infection in either the arthropod or mammalian host (59). Our findings thus suggest that the differences in LPS detection between TLR4 and Casp11 constrain the lipid A structures that can evade both components of innate immune LPS sensing. While downregulation of *lxpP* or *msbB* could allow *Y. pestis* to evade TLR4 or Casp11, respectively, the bacterium must downregulate both to generate a tetra-acylated lipid A within a mammalian host. While *Y. pestis* has been able to evolve such a mechanism, generation of tetra-acylated lipid A comes with a strong fitness cost. *Y. pestis* strains grown at 37°C or lacking *msbB* and *lpxP* are more susceptible to cationic antimicrobial peptides (47, 50). Indeed, other Gram-negative *Enterobacteriaceae* that are engineered to produce tetra-acylated LPS structures are generally attenuated for growth and highly sensitive to environmental perturbation (60). Increased susceptibility to cationic antimicrobials and other environmental stressors for bacteria that produce underacylated LPS molecules thus highlights the selective pressure that these LPS receptors place on Gram-negative pathogens.

Lipid A structures that do not stimulate either TLR4 or Casp11 have been isolated from nonpathogenic organisms that reside in deep sea environments (61). However, these lipid A structures appear to avoid detection without needing to be hypo-acylated, possibly by sampling areas of lipid A chemical space that cannot be readily accessed by pathogens at the temperatures and environmental pressures found in terrestrial environments or in mammalian hosts (61). Interestingly, mouse Casp11 and human Casp4/5 are sensitive to distinct lipid A structures, as the human noncanonical inflammasome can detect hypo-acylated lipid A species that fail to activate Casp11 (51). Consistently, Casp4/5 do not distinguish between different species of penta-acylated lipid A in the way that Casp11 does (54). However, human TLR4 is less sensitive to hypo-acylated LPS than mouse TLR4 (30). Altogether, our findings described here and by Alexander-Floyd et al. (54) highlight the complementary recognition mechanisms displayed by both human and mouse cytosolic and cell surface LPS sensing pathways. While there are unique structures detected by all four systems, our findings collectively indicate that each single host species possesses a self-contained endotoxin sensing pathway that comprehensively surveys lipid A structures and limits the capacity of microbial pathogens to evade detection.

MATERIALS AND METHODS

Bacterial strains and lipid A extraction. The bacterial strains used in these studies were created in the laboratory of B. Joseph Hinnebusch and were previously described in Rebeil et al. (50). Bacteria were cultured in brain heart infusion (BHI) medium (BD Biosciences; catalog no. 237200) prepared according to the manufacturer's recommendation and supplemented with 1 mM $MgCl_2$. Briefly, overnight cultures (10 mL) were grown with shaking (200 rpm) at 26°C and used to inoculate 1-L liquid cultures which were grown for 18 to 24 h under the same conditions (53). Bacterial pellets were harvested by centrifuging at 10,000 $\times$ *g* for 20 min.

Extraction of LOS was performed as previously described (53) with the modifications noted below. A hot phenol extraction was then performed by resuspending the resultant pellet from 1 L of culture in 60 mL endotoxin-free water. This suspension was split evenly among three 50-mL conical tubes, and an equal volume (20 mL) of 90% phenol was added to each tube, and the tubes were incubated at 65°C for 1 h with intermittent vortexing. The mixture was cooled on ice for 5 min and centrifuged at 3,000 $\times$ *g* for 20 min at room temperature (RT). The aqueous (top) layer was removed and placed into a new 50-mL conical tube. An equal volume of endotoxin-free water was added to the original tube, and the extraction steps were repeated. The two aqueous layers were combined and dialyzed using 1-kDa molecular weight cutoff (MWCO) tubing (Spectrum Laboratories; catalog no. 132105) for 24 to 36 h at 4°C in at least 4 L of double-distilled water (ddH_2O). The ddH_2O was changed several times during the dialysis period. To remove any remaining insoluble material, the aqueous solution was centrifuged at 5,000 $\times$ *g* for 20 min at RT, and the solution was lyophilized. The dried material was resuspended in 10 mL of 10 mM Tris-HCl (pH 7.4), and then 25 μg/mL RNase (Qiagen; catalog no. 19101) and 100 μg/mL of DNase I (Roche; catalog no. 10104159001) were added, followed by a 2- h incubation at 37°C. Then, 100 μg/mL of proteinase K (Invitrogen; catalog no. 25530-015) was then added, and the incubation continued at 37°C for an additional 2 h. Next, 5 mL of water-saturated phenol was added before the solution was mixed via vortex and then centrifuged at 3,000 $\times$ *g* for 20 min at RT. The resulting aqueous fraction was dialyzed for at least 12 h, and the insoluble fraction removed, and lyophilized as before, resulting in

extracted bacterial LOS. The product was further purified as previously described using chloroform/methanol washes to ensure removal of hydrophilic lipids and reextraction to remove any remaining lipoproteins (53, 62). Mild acid hydrolysis was carried out as previously described to further convert LOS to lipid A (53).

Cell culture. Reporter cell lines hTLR4 HEK-Blue (InvivoGen) and RAW-Blue (InvivoGen) were cultured in Dulbecco's modified Eagle's medium (DMEM) supplemented with 10% FBS, 100 U/mL penicillin-streptomycin, and 2 mM L-glutamine in a humidified tissue culture incubator at 37°C and 5% CO_2. Cells were split into a 96-well flat-bottom plate, allowed 24 to 48 h to adhere, and then stimulated with agonists over a 5-log concentration range. After 18 h of culture with agonist, 20 μL of cell culture supernatant was added to 180 μL of Quanti-Blue detection medium (InvivoGen) and developed in the tissue culture incubator for 20 min. The optical density (OD) at 620 nm was determined using a DTX 880 multimode plate reader (Beckman Coulter, Brea, CA). Mouse BMDMs were cultured in DMEM supplemented with 10% FBS, 10 mM HEPES, 1 mM sodium pyruvate, and 30% L929 cell-conditioned medium. Cells were grown for 6 to 7 days in petri plates before being reseeded into 48-well plates at 16 to 20 h before LOS or lipid A treatment.

LOS and lipid A intracellular delivery. For LOS transfection, mouse BMDMs were primed for 4 h with 400 ng/mL Pam3CSK4 in DMEM plus 10% L929 supernatant and then transfected with the indicated doses of endotoxin with 0.2% FuGENE HD in Opti-MEM. Then, 20 h after transfection, cell supernatants were assayed for cell death and cytokine concentrations. *L. monocytogenes*-mediated delivery of LOS was performed as previously described (34). Briefly, BMDMs were primed with 1 μg/mL high-molecular-weight (HMW) poly(I·C) for 16 h and then infected with *L. monocytogenes* strain 10403S at a multiplicity of infection (MOI) of 5 in the presence of LOS. One hour after infection, the medium was replaced with medium containing 20 μg/mL gentamicin. Four hours after infection, cell supernatants were harvested to quantify cell death. For both methods of intracellular delivery, cell death was assayed using a lactate dehydrogenase release assay kit (TaKaRa Bio) according to the manufacturer's instructions.

Cytokine analysis. Cytokine levels in bone marrow derived macrophage supernatants were measured using a custom cytometric bead array Flex set (BD Biosciences) according to the manufacturer's specifications. Bead and supernatant mixtures were incubated for 1.5 h at 25°C at 600 rpm in 96-well V-bottom plates. Samples were then washed using fluorescence-activated cell sorter (FACS) wash buffer (1× phosphate-buffered saline [PBS] plus 2% FBS plus 0.05% [wt/vol] sodium azide). All data were collected on an LSRFortessa instrument (BD Biosciences) and analyzed using FlowJo software by gating on individual bead populations and calculating the geometric mean of fluorescence relative to purified protein standards.

IL-1β ELISA. Supernatants were applied, along with recombinant cytokine standards, to Immulon enzyme-linked immunosorbent assay (ELISA) plates (ImmunoChemistry Technologies) that were precoated with anti-IL-1β capture antibody (eBioscience). IL-1β was then detected with a secondary biotinylated antibody (eBioscience) followed by streptavidin conjugated to horseradish peroxidase (BD Biosciences). Peroxidase activity was detected by o-phenylenediamine hydrochloride (Sigma-Aldrich) in citrate buffer. Reactions were stopped with sulfuric acid and read at 490 nm.

Western blots. BMDM lysates and supernatants were harvested for immunoblotting 20 h following lipid A transfection, as previously described (63). Briefly, supernatants were cleared of cell debris by centrifugation and incubated with 0.61 N trichloroacetic acid (TCA; Sigma-Aldrich) plus 1× protease inhibitory cocktail (PIC; Sigma-Aldrich) for at least 1 h at 4°C. Precipitates were then isolated and washed with acetone by repeated centrifugation at 4°C. The resulting protein pellet was resuspended in protein sample buffer (125 mM Tris, 10% SDS, 50% glycerol, 0.06% bromophenol blue, 1% β-mercaptoethanol, 50 mM dithiothreitol) and analyzed by SDS-PAGE. BMDM lysates were harvested in lysis buffer (20 mM HEPES, 150 mM NaCl, 10% glycerol, 1% Triton X-100, 1 mM EDTA, pH 7.5) supplemented with 1× PIC and 1× protein sample buffer and rocked gently for 10 min at 4°C. Protein samples from lysates and supernatants were boiled, centrifuged at full speed for 5 min, run on 4 to 12% polyacrylamide gels (Invitrogen), and then transferred to polyvinylidene difluoride (PVDF) membranes. Membranes were immunoblotted using the following primary antibodies: β-actin (1:2,500; Sigma-Aldrich AC74), Casp11 (1:1,000; Novus Biologicals 17D9), and GSDMD (1:500; Abcam EPR19828). Species-specific horseradish peroxidase-conjugated secondary antibodies (1:2,500) were used for each antibody. Blots were developed by chemiluminescence using Pierce SuperSignal West femto maximum sensitivity substrate (Thermo Scientific) according to the manufacturer's instructions.

Graphs and statistics. Data were graphed and statistical analyses performed in GraphPad Prism 8.4.3 (San Diego, CA). Statistically significant differences between experimental conditions were determined by multiple *t* tests using the Holm-Sidak method. Best-fit lines were calculated in Prism using an equation for 4-parameter variable slope regressions.

SUPPLEMENTAL MATERIAL

Supplemental material is available online only.

SUPPLEMENTAL FILE 1, PDF file, 0.1 MB.

ACKNOWLEDGMENTS

We thank members of the Brodsky, Shin, and Ernst laboratories for helpful scientific discussions.

This work is supported in part by NIH grants R01AI128530 and R01AI139102A1 (I.E.B.), NIH grants R01AI118861 and R01AI123243 (S.S.), HHS-NIH-NIAID-BAA2017 (R.K.E.), NIH training grants T32AI095190 (E.M.H.), and T32 AR076951 (D.G.) and a Burroughs-Welcome Fund Investigators in the Pathogenesis of Infectious Diseases Award (I.E.B. and S.S.).

REFERENCES

1. Weiss J, Barker J. 2018. Diverse pro-inflammatory endotoxin recognition systems of mammalian innate immunity. F1000Res 7:516. https://doi.org/10.12688/f1000research.13977.1.
2. Hoshino K, Takeuchi O, Kawai T, Sanjo H, Ogawa T, Takeda Y, Takeda K, Akira S. 1999. Cutting edge: Toll-like receptor 4 (TLR4)-deficient mice are hyporesponsive to lipopolysaccharide: evidence for TLR4 as the Lps gene product. J Immunol 162:3749–3752.
3. Wang S, Miura M, Jung YK, Zhu H, Li E, Yuan J. 1998. Murine caspase-11, an ICE-interacting protease, is essential for the activation of ICE. Cell 92:501–509. https://doi.org/10.1016/s0092-8674(00)80943-5.
4. Kayagaki N, Wong MT, Stowe IB, Ramani SR, Gonzalez LC, Akashi-Takamura S, Miyake K, Zhang J, Lee WP, Muszyński A, Forsberg LS, Carlson RW, Dixit VM. 2013. Noncanonical inflammasome activation by intracellular LPS independent of TLR4. Science 341:1246–1249. https://doi.org/10.1126/science.1240248.
5. Kang R, Zeng L, Zhu S, Xie Y, Liu J, Wen Q, Cao L, Xie M, Ran Q, Kroemer G, Wang H, Billiar TR, Jiang J, Tang D. 2018. Lipid peroxidation drives gasdermin D-mediated pyroptosis in lethal polymicrobial sepsis. Cell Host Microbe 24:97–108.e4. https://doi.org/10.1016/j.chom.2018.05.009.
6. Park BS, Song DH, Kim HM, Choi B-S, Lee H, Lee J-O. 2009. The structural basis of lipopolysaccharide recognition by the TLR4-MD-2 complex. Nature 458:1191–1195. https://doi.org/10.1038/nature07830.
7. Shi J, Zhao Y, Wang Y, Gao W, Ding J, Li P, Hu L, Shao F. 2014. Inflammatory caspases are innate immune receptors for intracellular LPS. Nature 514:187–192. https://doi.org/10.1038/nature13683.
8. Xiao X, Sankaranarayanan K, Khosla C. 2017. Biosynthesis and structure-activity relationships of the lipid a family of glycolipids. Curr Opin Chem Biol 40:127–137. https://doi.org/10.1016/j.cbpa.2017.07.008.
9. Raetz CRH, Reynolds CM, Trent MS, Bishop RE. 2007. Lipid A modification systems in Gram-negative bacteria. Annu Rev Biochem 76:295–329. https://doi.org/10.1146/annurev.biochem.76.010307.145803.
10. Chilton PM, Embry CA, Mitchell TC. 2012. Effects of differences in lipid A structure on TLR4 pro-inflammatory signaling and inflammasome activation. Front Immunol 3:154.
11. Park BS, Lee JO. 2013. Recognition of lipopolysaccharide pattern by TLR4 complexes. Exp Mol Med 45:e66. https://doi.org/10.1038/emm.2013.97.
12. Kawasaki T, Kawai T. 2014. Toll-like receptor signaling pathways. Front Immunol 5:461. https://doi.org/10.3389/fimmu.2014.00461.
13. Maeshima N, Fernandez RC. 2013. Recognition of lipid A variants by the TLR4-MD-2 receptor complex. Front Cell Infect Microbiol 3:3.
14. Coats SR, Pham T-TT, Bainbridge BW, Reife RA, Darveau RP. 2005. MD-2 mediates the ability of tetra-acylated and penta-acylated lipopolysaccharides to antagonize Escherichia coli lipopolysaccharide at the TLR4 signaling complex. J Immunol 175:4490–4498. https://doi.org/10.4049/jimmunol.175.7.4490.
15. Steimle A, Autenrieth IB, Frick JS. 2016. Structure and function: lipid A modifications in commensals and pathogens. Int J Med Microbiol 306:290–301. https://doi.org/10.1016/j.ijmm.2016.03.001.
16. Jones BD, Nichols WA, Gibson BW, Sunshine MG, Apicella MA. 1997. Study of the role of the htrB gene in Salmonella Typhimurium virulence. Infect Immun 65:4778–4783. https://doi.org/10.1128/iai.65.11.4778-4783.1997.
17. Sunshine MG, Gibson BW, Engstrom JJ, Nichols WA, Jones BD, Apicella MA. 1997. Mutation of the htrB gene in a virulent Salmonella Typhimurium strain by intergeneric transduction: strain construction and phenotypic characterization. J Bacteriol 179:5521–5533. https://doi.org/10.1128/jb.179.17.5521-5533.1997.
18. Vaara M, Nurminen M. 1999. Outer membrane permeability barrier in Escherichia coli mutants that are defective in the late acyltransferases of lipid A biosynthesis. Antimicrob Agents Chemother 43:1459–1462. https://doi.org/10.1128/AAC.43.6.1459.
19. Ellis CD, Lindner B, Anjam Khan CM, Zähringer U, Demarco de Hormaeche R. 2001. The Neisseria gonorrhoeae lpxLII gene encodes for a late-functioning lauroyl acyl transferase, and a null mutation within the gene has a significant effect on the induction of acute inflammatory responses. Mol Microbiol 42:167–181. https://doi.org/10.1046/j.1365-2958.2001.02619.x.
20. van der Ley P, Steeghs L, Hamstra HJ, ten Hove J, Zomer B, van Alphen L. 2001. Modification of lipid A biosynthesis in Neisseria meningitidis lpxL mutants: influence on lipopolysaccharide structure, toxicity, and adjuvant activity. Infect Immun 69:5981–5990. https://doi.org/10.1128/IAI.69.10.5981-5990.2001.
21. Tong HH, Chen Y, James M, Van Deusen J, Welling DB, DeMaria TF. 2001. Expression of cytokine and chemokine genes by human middle ear epithelial cells induced by formalin-killed Haemophilus influenzae or its lipooligosaccharide htrB and rfaD mutants. Infect Immun 69:3678–3684. https://doi.org/10.1128/IAI.69.6.3678-3684.2001.
22. Post DMB, Phillips NJ, Shao JQ, Entz DD, Gibson BW, Apicella MA. 2002. Intracellular survival of Neisseria gonorrhoeae in male urethral epithelial cells: importance of a hexaacyl lipid A. Infect Immun 70:909–920. https://doi.org/10.1128/IAI.70.2.909-920.2002.
23. Ingram BO, Sohlenkamp C, Geiger O, Raetz CRH. 2010. Altered lipid A structures and polymyxin hypersensitivity of Rhizobium etli mutants lacking the LpxE and LpxF phosphatases. Biochim Biophys Acta 1801:593–604. https://doi.org/10.1016/j.bbalip.2010.02.001.
24. Cullen TW, Giles DK, Wolf LN, Ecobichon C, Boneca IG, Trent MS. 2011. Helicobacter pylori versus the host: remodeling of the bacterial outer membrane is required for survival in the gastric mucosa. PLoS Pathog 7:e1002454. https://doi.org/10.1371/journal.ppat.1002454.
25. Kong Q, Six DA, Liu Q, Gu L, Wang S, Alamuri P, Raetz CRH, Curtiss R. 2012. Phosphate groups of lipid A are essential for Salmonella enterica serovar Typhimurium virulence and affect innate and adaptive immunity. Infect Immun 80:3215–3224. https://doi.org/10.1128/IAI.00123-12.
26. Wang X, McGrath SC, Cotter RJ, Raetz CRH. 2006. Expression cloning and periplasmic orientation of the Francisella novicida lipid A 4′-phosphatase LpxF. J Biol Chem 281:9321–9330. https://doi.org/10.1074/jbc.M600435200.
27. Jones JW, Cohen IE, Tureček F, Goodlett DR, Ernst RK. 2010. Comprehensive structure characterization of lipid A extracted from Yersinia pestis for determination of its phosphorylation configuration. J Am Soc Mass Spectrom 21:785–799. https://doi.org/10.1016/j.jasms.2010.01.008.
28. Guo L, Lim KB, Poduje CM, Daniel M, Gunn JS, Hackett M, Miller SI. 1998. Lipid A acylation and bacterial resistance against vertebrate antimicrobial peptides. Cell 95:189–198. https://doi.org/10.1016/S0092-8674(00)81750-X.
29. Coats SR, Jones JW, Do CT, Braham PH, Bainbridge BW, To TT, Goodlett DR, Ernst RK, Darveau RP. 2009. Human Toll-like receptor 4 responses to P gingivalis are regulated by lipid A 1- and 4'-phosphatase activities. Cell Microbiol 11:1587–1599. https://doi.org/10.1111/j.1462-5822.2009.01349.x.
30. Vaure C, Liu Y. 2014. A comparative review of toll-like receptor 4 expression and functionality in different animal species. Front Immunol 5:316.
31. Hajjar AM, Ernst RK, Tsai JH, Wilson CB, Miller SI. 2002. Human Toll-like receptor 4 recognizes host-specific LPS modifications. Nat Immunol 3:354–359. https://doi.org/10.1038/ni777.
32. Kawahara K, Tsukano H, Watanabe H, Lindner B, Matsuura M. 2002. Modification of the structure and activity of lipid A in Yersinia pestis lipopolysaccharide by growth temperature. Infect Immun 70:4092–4098. https://doi.org/10.1128/IAI.70.8.4092-4098.2002.
33. Aachoui Y, Leaf IA, Hagar JA, Fontana MF, Campos CG, Zak DE, Tan MH, Cotter PA, Vance RE, Aderem A, Miao EA. 2013. Caspase-11 protects against bacteria that escape the vacuole. Science 339:975–978. https://doi.org/10.1126/science.1230751.
34. Hagar JA, Powell DA, Aachoui Y, Ernst RK, Miao EA. 2013. Cytoplasmic LPS activates caspase-11: implications in TLR4-independent endotoxic shock. Science 341:1250–1253. https://doi.org/10.1126/science.1240988.
35. Kayagaki N, Warming S, Lamkanfi M, Vande Walle L, Louie S, Dong J, Newton K, Qu Y, Liu J, Heldens S, Zhang J, Lee WP, Roose-Girma M, Dixit VM. 2011. Non-canonical inflammasome activation targets caspase-11. Nature 479:117–121. https://doi.org/10.1038/nature10558.
36. Meunier E, Dick MS, Dreier RF, Schürmann N, Kenzelmann Broz D, Warming S, Roose-Girma M, Bumann D, Kayagaki N, Takeda K, Yamamoto M, Broz P.

2014. Caspase-11 activation requires lysis of pathogen-containing vacuoles by IFN-induced GTPases. Nature 509:366–370. https://doi.org/10.1038/nature13157.
37. Santos JC, Boucher D, Schneider LK, Demarco B, Dilucca M, Shkarina K, Heilig R, Chen KW, Lim RYH, Broz P. 2020. Human GBP1 binds LPS to initiate assembly of a caspase-4 activating platform on cytosolic bacteria. Nat Commun 11:3276. https://doi.org/10.1038/s41467-020-16889-z.
38. Pilla DM, Hagar JA, Haldar AK, Mason AK, Degrandi D, Pfeffer K, Ernst RK, Yamamoto M, Miao EA, Coers J. 2014. Guanylate binding proteins promote caspase-11-dependent pyroptosis in response to cytoplasmic LPS. Proc Natl Acad Sci U S A 111:6046–6051. https://doi.org/10.1073/pnas.1321700111.
39. Wandel MP, Kim B-H, Park E-S, Boyle KB, Nayak K, Lagrange B, Herod A, Henry T, Zilbauer M, Rohde J, MacMicking JD, Randow F. 2020. Guanylate-binding proteins convert cytosolic bacteria into caspase-4 signaling platforms. Nat Immunol 21:880–891. https://doi.org/10.1038/s41590-020-0697-2.
40. Lee BL, Stowe IB, Gupta A, Kornfeld OS, Roose-Girma M, Anderson K, Warming S, Zhang J, Lee WP, Kayagaki N. 2018. Caspase-11 auto-proteolysis is crucial for noncanonical inflammasome activation. J Exp Med 215:2279–2288. https://doi.org/10.1084/jem.20180589.
41. Kayagaki N, Stowe IB, Lee BL, O'Rourke K, Anderson K, Warming S, Cuellar T, Haley B, Roose-Girma M, Phung QT, Liu PS, Lill JR, Li H, Wu J, Kummerfeld S, Zhang J, Lee WP, Snipas SJ, Salvesen GS, Morris LX, Fitzgerald L, Zhang Y, Bertram EM, Goodnow CC, Dixit VM. 2015. Caspase-11 cleaves gasdermin D for non-canonical inflammasome signalling. Nature 526:666–671. https://doi.org/10.1038/nature15541.
42. Shi J, Zhao Y, Wang K, Shi X, Wang Y, Huang H, Zhuang Y, Cai T, Wang F, Shao F. 2015. Cleavage of GSDMD by inflammatory caspases determines pyroptotic cell death. Nature 526:660–665. https://doi.org/10.1038/nature15514.
43. Kim HM, Park BS, Kim J-I, Kim SE, Lee J, Oh SC, Enkhbayar P, Matsushima N, Lee H, Yoo OJ, Lee J-O. 2007. Crystal structure of the TLR4-MD-2 complex with bound endotoxin antagonist Eritoran. Cell 130:906–917. https://doi.org/10.1016/j.cell.2007.08.002.
44. Prior JL, Parkhill J, Hitchen PG, Mungall KL, Stevens K, Morris HR, Reason AJ, Oyston PC, Dell A, Wren BW, Titball RW. 2001. The failure of different strains of Yersinia pestis to produce lipopolysaccharide O-antigen under different growth conditions is due to mutations in the O-antigen gene cluster. FEMS Microbiol Lett 197:229–233. https://doi.org/10.1111/j.1574-6968.2001.tb10608.x.
45. Scott AJ, Oyler BL, Goodlett DR, Ernst RK. 2017. Lipid A structural modifications in extreme conditions and identification of unique modifying enzymes to define the Toll-like receptor 4 structure-activity relationship. Biochim Biophys Acta Mol Cell Biol Lipids 1862:1439–1450. https://doi.org/10.1016/j.bbalip.2017.01.004.
46. Vadyvaloo V, Jarrett C, Sturdevant DE, Sebbane F, Hinnebusch BJ. 2010. Transit through the flea vector induces a pretransmission innate immunity resistance phenotype in Yersinia pestis. PLoS Pathog 6:e1000783. https://doi.org/10.1371/journal.ppat.1000783.
47. Rebeil R, Ernst RK, Gowen BB, Miller SI, Hinnebusch BJ. 2004. Variation in lipid A structure in the pathogenic yersiniae. Mol Microbiol 52:1363–1373. https://doi.org/10.1111/j.1365-2958.2004.04059.x.
48. Montminy SW, Khan N, McGrath S, Walkowicz MJ, Sharp F, Conlon JE, Fukase K, Kusumoto S, Sweet C, Miyake K, Akira S, Cotter RJ, Goguen JD, Lien E. 2006. Virulence factors of Yersinia pestis are overcome by a strong lipopolysaccharide response. Nat Immunol 7:1066–1073. https://doi.org/10.1038/ni1386.
49. Hajjar AM, Ernst RK, Fortuno ES, Brasfield AS, Yam CS, Newlon LA, Kollmann TR, Miller SI, Wilson CB. 2012. Humanized TLR4/MD-2 mice reveal LPS recognition differentially impacts susceptibility to Yersinia pestis and Salmonella enterica. PLoS Pathog 8:e1002963. https://doi.org/10.1371/journal.ppat.1002963.
50. Rebeil R, Ernst RK, Jarrett CO, Adams KN, Miller SI, Hinnebusch BJ. 2006. Characterization of late acyltransferase genes of Yersinia pestis and their role in temperature-dependent lipid A variation. J Bacteriol 188:1381–1388. https://doi.org/10.1128/JB.188.4.1381-1388.2006.
51. Lagrange B, Benaoudia S, Wallet P, Magnotti F, Provost A, Michal F, Martin A, Di Lorenzo F, Py BF, Molinaro A, Henry T. 2018. Human caspase-4 detects tetra-acylated LPS and cytosolic Francisella and functions differently from murine caspase-11. Nat Commun 9:242. https://doi.org/10.1038/s41467-017-02682-y.
52. Ernst O, Khan MM, Oyler BL, Yoon SH, Sun J, Lin F-Y, Manes NP, MacKerell AD, Fraser IDC, Ernst RK, Goodlett DR, Nita-Lazar A. 2021. Species-specific endotoxin stimulus determines Toll-like receptor 4- and caspase 11-mediated pathway activation characteristics. mSystems 6:e0030621. https://doi.org/10.1128/mSystems.00306-21.
53. Gregg KA, Harberts E, Gardner FM, Pelletier MR, Cayatte C, Yu L, McCarthy MP, Marshall JD, Ernst RK. 2017. Rationally designed TLR4 ligands for vaccine adjuvant discovery. mBio 8:e00492-17. https://doi.org/10.1128/mBio.00492-17.
54. Alexander-Floyd J, Bass AR, Harberts EM, Grubaugh D, Buxbaum J, Brodsky IE, Ernst RK, Shina S. 2022. Lipid A variants activate human TLR4 and the noncanonical inflammasome differently and require the core oligosaccharide for inflammasome activation. Infect Immun https://doi.org/10.1128/iai.00208-22.
55. Preston A, Mandrell RE, Gibson BW, Apicella MA. 1996. The lipooligosaccharides of pathogenic gram-negative bacteria. Crit Rev Microbiol 22:139–180. https://doi.org/10.3109/10408419609106458.
56. Carlson RW, Forsberg LS, Kannenberg EL. 2010. Lipopolysaccharides in Rhizobium-legume symbioses. Subcell Biochem 53:339–386. https://doi.org/10.1007/978-90-481-9078-2_16.
57. Muszynski A, Laus M, Kijne JW, Carlson RW. 2011. Structures of the lipopolysaccharides from Rhizobium leguminosarum RBL5523 and its UDP-glucose dehydrogenase mutant (exo5). Glycobiology 21:55–68. https://doi.org/10.1093/glycob/cwq131.
58. Yang C, Briones M, Chiou J, Lei L, Patton MJ, Ma L, McClarty G, Caldwell HD. 2019. Chlamydia trachomatis lipopolysaccharide evades the canonical and noncanonical inflammatory pathways to subvert innate immunity. mBio 10:e00595-19. https://doi.org/10.1128/mBio.00595-19.
59. Demeure CE, Dussurget O, Mas Fiol G, Le Guern A-S, Savin C, Pizarro-Cerdá J. 2019. Yersinia pestis and plague: an updated view on evolution, virulence determinants, immune subversion, vaccination, and diagnostics. Genes Immun 20:357–370. https://doi.org/10.1038/s41435-019-0065-0.
60. Vorachek-Warren MK, Ramirez S, Cotter RJ, Raetz CRH. 2002. A triple mutant of Escherichia coli lacking secondary acyl chains on lipid A. J Biol Chem 277:14194–14205. https://doi.org/10.1074/jbc.M200409200.
61. Gauthier AE, Chandler CE, Poli V, Gardner FM, Tekiau A, Smith R, Bonham KS, Cordes EE, Shank TM, Zanoni I, Goodlett DR, Biller SJ, Ernst RK, Rotjan RD, Kagan JC. 2021. Deep-sea microbes as tools to refine the rules of innate immune pattern recognition. Sci Immunol 57:eabe0531. https://doi.org/10.1126/sciimmunol.abe0531.
62. Hirschfeld M, Ma Y, Weis JH, Vogel SN, Weis JJ. 2000. Cutting edge: repurification of lipopolysaccharide eliminates signaling through both human and murine toll-like receptor 2. J Immunol 165:618–622. https://doi.org/10.4049/jimmunol.165.2.618.
63. Bjanes E, Sillas RG, Matsuda R, Demarco B, Fettrelet T, DeLaney AA, Kornfeld OS, Lee BL, Rodríguez López EM, Grubaugh D, Wynosky-Dolfi MA, Philip NH, Krespan E, Tovar D, Joannas L, Beiting DP, Henao-Mejia J, Schaefer BC, Chen KW, Broz P, Brodsky IE. 2021. Genetic targeting of Card19 is linked to disrupted NINJ1 expression, impaired cell lysis, and increased susceptibility to Yersinia infection. PLoS Pathog 17:e1009967. https://doi.org/10.1371/journal.ppat.1009967.